

The effect of substituent groups on the reductive degradation of azo dyes by zerovalent iron

Meifang Hou, Fangbai Li*, Xinming Liu, Xugang Wang, Hongfu Wan

Guangdong Key Laboratory of Agricultural Environment Pollution Integrated Control,
Guangdong Institute of Eco-Environmental and Soil Sciences, 510650 Guangzhou, China

Received 25 July 2006; received in revised form 12 November 2006; accepted 13 November 2006
Available online 18 November 2006

Abstract

To investigate the effects of substituent groups on the reductive degradation of azo dyes by zerovalent iron, Orange I, Orange II and Methyl Orange were selected as the model azo dyes with different substituent groups. The results showed that Orange I, Orange II and Methyl Orange could be effectively reduced by Fe^0 , and the degradation of Orange I and Orange II could be described by the first-order kinetic model, while the degradation of Methyl Orange could be described by the zeroth-order kinetic model. The initial degradation rate followed the order as Orange I > Orange II > Methyl Orange under the same experimental conditions owing to the substituent effects. The degradation kinetic constants of Orange I and Orange II increased with the increase in the Fe^0 dosage, and with the decrease in the initial pH value and their initial concentration, while that of Methyl Orange increased with the decrease in the initial pH value, and with the increase in the Fe^0 dosage and their initial concentration. The results of high-performance liquid chromatography (HPLC)–mass spectra (MS) showed that sulfanilic acid was the same intermediate, while the second intermediate was 1-amino-4-naphthol for Orange I, 1-amino-2-naphthol for Orange II, and *p*-dimethylaminoaniline for Methyl Orange. It was suggested that the larger conjugated π system of naphthalene rings of Orange I and Orange II for the delocalization of the nonbonding electron pairs of substituents and nitrogen in the azo bond might be favorable for the degradation of Orange I and Orange II, compared with the structure of Methyl Orange. The higher degradation rate of Orange I might be ascribed to its effective electron delocalization and favorable position effects, compared with Orange II. It should be concluded that the reductive degradation of azo dyes by zerovalent iron strongly depends on the effect of substituent groups.

© 2006 Elsevier B.V. All rights reserved.

Keywords: Azo dye; Zerovalent iron; Reductive degradation; Substituent effect

1. Introduction

Azo dyes are widely used in the textile, paper, plastic, leather, food, cosmetic and pharmaceutical industries [1–3]. The effluents of azo dyes lead to the environmental pollution. The removal methods of dyes include physical adsorption, oxidation or reduction methods, and biological degradation, or the integrative treatments of various methods. Among them, the reductive degradation of azo dyes by zerovalent iron (Fe^0) has been paid much attention in recent years [3–5].

Orange I, Orange II as well as Methyl Orange are common azo dye pollutants in the environment, which were usually chosen as the model azo dyes in the literatures [1–12]. In recent years,

the degradation of Orange II by zerovalent iron has been studied extensively [3,5]. For examples, Zhang et al. [5] investigated the effect of ultrasound on the enhancement of the degradation of Orange II by Fe^0 , and they found that the degradation of Orange II under the synergic treatment of Fe^0 and ultrasound radiation followed the first-order kinetic model. Mielczarski et al. [3] focused on the role of iron surface oxidation layers in the degradation of Orange II and Orange I in weak acidic solutions, and they suggested that iron surface layer composition and structure might influence the reduction rate of Orange II and Orange I by Fe^0 . The azo group of dyes is usually conjugated with hydroxyl groups or other electron-donating groups, which play an important role in the reduction mechanisms [2]. The degradability of various substituted sulfonated azo dyes was investigated, and it was reported that the effect of substituents on the degradability of azo dyes should depend strongly on the differences between the electron-donating substituent groups

* Corresponding author. Tel.: +86 20 87024721; fax: +86 20 87024123.
E-mail address: cefbli@soil.gd.cn (F. Li).

and the electron-withdrawing substituent groups [6]. It was also reported that the $-\text{N}(\text{CH}_3)_2$ group of Methyl Orange might be the important site of photodegradation attack, while the $-\text{OH}$ group in the naphthol moiety of Orange II may be an obstacle to subsequent hydroxylation reactions [8]. Consequently, chemical structure and substituent group of azo dyes should significantly influence the degradation pathway and the degradation kinetics. Even though the degradation of azo dyes by Fe^0 has attracted much attention, there are few reports about the effects of substituent groups on the degradation kinetics and mechanisms of azo dyes by zerovalent iron.

The main objective of this investigation is to study the effects of different substituent groups on the degradation of azo dyes by Fe^0 . Orange I and Methyl Orange were selected as the model azo dyes with the different substituent groups, and Orange II was also studied as the isomer of Orange I in the paper. The effects of the initial concentration of azo dyes, the initial pH value and the Fe^0 dosage on the degradation kinetics were also further investigated to disclose the effect of substituent groups. The work may provide a new insight into the degradation of azo dyes by zerovalent iron.

2. Experimental methods

2.1. Materials and chemicals

The zerovalent iron (Fe^0) powder with the particle size of 100 mesh and 99.9% purity was purchased from Tianjin Kermel Chemical Reagent Development Center, Tianjin, China, without any further purification. Its specific surface area measured by BET analysis was $7.5 \text{ m}^2 \text{ g}^{-1}$. Methyl Orange, Orange I and Orange II were purchased from Aldrich. Other chemicals including HCl and NaOH were obtained in China with analytical grade and were used without further purification. The chemical structures of the model azo dyes are shown in Fig. 1.

2.2. Batch experiments by Fe^0

The batch experiments were carried out in a 250 mL flask under N_2 gas at room temperature. The reaction of azo dyes with Fe^0 was investigated under different factors, including the initial concentration of azo dyes, the initial pH value and the Fe^0 dosage. The initial pH value in the solution of azo dyes was adjusted by HCl and NaOH. For all experiments, the 200 mL solution of azo dyes at the desired pH was firstly purged with N_2 for 30 min, and then put the Fe^0 powder into the reaction solution under the vigorous stirring. N_2 gas was continuously bubbling to keep the free oxygen state. The samples were taken at different time intervals and then separated by centrifugation at 4500 rpm for 30 min to get the supernatant and the sediment for analysis. If specification, the experiments were done in the dark.

To investigate the effect of the initial pH value for the degradation of azo dyes with different substituents, the pH value of 2.0, 4.0, 5.0, 6.0, 7.0 or 7.2 were used in the experiments. To investigate the effect of initial concentration of azo dyes, the experiments were carried out in the presence of the initial con-

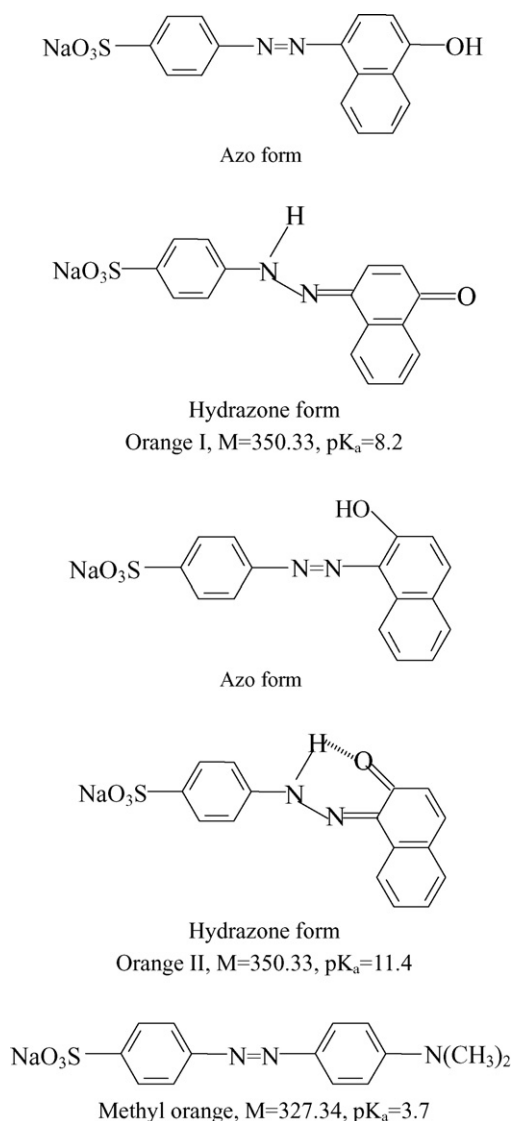


Fig. 1. The chemical structures of Orange I, Orange II and Methyl Orange.

centration at 20, 50, 100, 150, 200 or 300 mg L^{-1} . To investigate the effect of Fe^0 dosage, the experiments were conducted with the Fe^0 dosage of 1, 2, 3, 4 or 5 g L^{-1} in this paper.

2.3. UV-vis absorption spectra, FTIR and HPLC/MS analyses

The concentrations of Orange I, Orange II and Methyl Orange were quantified by UV-vis spectrophotometry (TU1800-PC, Beijing) and the UV-vis absorption spectra of the aqueous solutions were also recorded. The measurements should be carried out as soon as possible after each sampling. Reaction solution was diluted five times before measurement to record spectra in most adsorbance region and the standard curve was modified according to the pH value of diluted reaction solution. The pH value was detected by the pH meter (pHS-3, Shanghai, China). FTIR spectra of the Fe^0 powder before and after reaction in the acidic condition for 2 h were recorded as KBr pellets in the

spectral range 4000–400 cm^{-1} on a Perkin-Elmer 1725X FT-IR spectrometer in air at room temperature.

The intermediates of azo dyes reduction by Fe^0 were analyzed by high-performance liquid chromatography (HPLC) using a Waters 600E system, equipped with a Model 486 variable wavelength UV detector set at 256 nm and a reverse-phase Waters Spherisorb column 4.6 mm \times 250 mm, equipped with a silica precolumn guard. Acetonitrile and 0.1 mol L^{-1} ammonium acetate filtered through a 0.2 μm filter were used as mobile phases at flow rates of 1 mL min^{-1} . From 0 to 5 min the ratio of acetonitrile:ammonium acetate was 1:1; from 5 to 10 min the ratio was 2:1. Analyses were evaluated using Millennium Version 3.20 software. During the analyses of high-performance liquid chromatography (HPLC)–mass spectra (MS), the reverse-phase column was coupled with Finnigan-MAT LCQ mass spectra via the Finnigan electrospray interface (Finnigan MAT, MAT, San Jose, CA, USA) operating in the positive or negative ion modes. The injection volume was 10 μL .

3. Results and discussion

3.1. The degradation of azo dyes by Fe^0

A series of experiments were carried out to investigate the degradation of azo dyes by Fe^0 with the initial concentration of 50 mg L^{-1} and the Fe^0 dosage of 5 g L^{-1} at pH 4.0, as shown in Fig. 2. The experimental results showed that the degradation of Orange I was much faster than those of Orange II and Methyl Orange under the same experimental conditions. The Langmuir–Hinshelwood model (L–H model) (Eq. (1)) is usually involved in the solid–liquid heterogeneous reaction kinetic, which might lead to the first-order kinetic model (Eq. (2)) and the zeroth-order kinetic model (Eq. (3)) when the value of KC is much less than 1.

$$-\frac{dC}{dt} = r = \frac{kKC}{1 + KC} \quad (1)$$

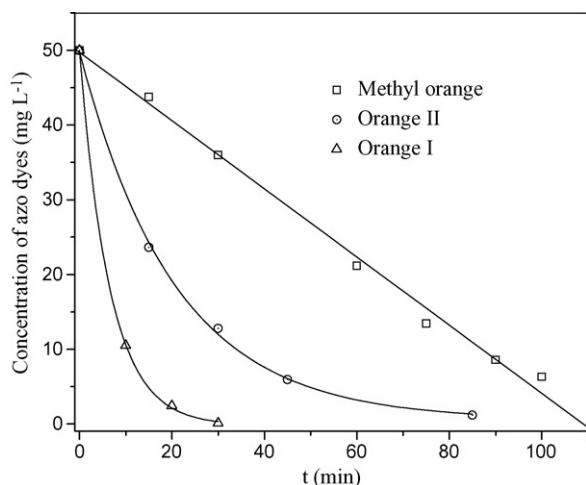


Fig. 2. The degradation of Orange I, Orange II and Methyl Orange by Fe^0 (initial concentration of dyes, 50 mg L^{-1} ; Fe^0 dosage, 2 g L^{-1} ; pH 4.0).

$$-\frac{dC}{dt} = r = kKC \quad (2)$$

$$-\frac{dC}{dt} = r = k \quad (3)$$

where r is the degradation rate of the organic substrate ($\text{mg L}^{-1} \text{min}^{-1}$), k the degradation kinetic constant (min^{-1} in Eq. (2) or $\text{mg L}^{-1} \text{min}^{-1}$ in Eq. (3)), K the adsorption equilibrium constant (L mg^{-1}), C the concentration of the substrate in the aqueous solution (mg L^{-1}) and t is the reaction time (min).

Generally, for a heterogeneous reaction occurring on the surface of catalysts, adsorption would be an important step to affect the degradation kinetics of azo dye during the reaction, since the catalysts can increase the overall reaction rate by lowering the activation energy for the rate determining step through the chemisorption of reactants on the surface of catalysts. However, the degradation of azo dyes by zerovalent iron is not a catalytic reaction rather than a reductive reaction, which depends on the zerovalent iron and the other reductants (Fe^{2+} , H_2 , etc.) derived from the corrosion of zerovalent iron in the reaction solution. In fact, it is very difficult to determine the adsorption of azo dyes on the surface Fe^0 because the adsorption and reductive reaction should occur simultaneously. Thus, the first-order kinetic model and the zeroth-order kinetic model have to be applied for describing the degradation kinetics in this investigation, on the basis of the experimental data. As shown in Fig. 2, the degradation of Orange I and Orange II could be described by the first-order kinetic model, while the degradation of Methyl Orange seems to follow the zeroth-order kinetic model. The first-order kinetic constants were $86.37 \times 10^{-3} \text{ min}^{-1}$ ($R=0.993$) and $65.20 \times 10^{-3} \text{ min}^{-1}$ ($R=0.996$) for Orange I and Orange II, respectively. In the mean time, the zeroth-order kinetic constant for Methyl Orange was $0.46 \text{ mg L}^{-1} \text{ min}^{-1}$ ($R=0.996$). To compare the experimental results, the initial degradation rates (r_0) of Orange I, Orange II and Methyl Orange were calculated and those were 4.32, 3.12 and $0.46 \text{ mg L}^{-1} \text{ min}^{-1}$, respectively, based on Eqs. (2) and (3). Obviously, the initial degradation rate followed the order as Orange I > Orange II > Methyl Orange.

3.2. Effect of the initial pH values

The effect of the initial pH value on the degradation of azo dyes by Fe^0 is shown in Fig. 3A for Orange I with the initial concentration of 100 mg L^{-1} and the Fe^0 dosage of 2 g L^{-1} ; in Fig. 3B for Orange II with the initial concentration of 50 mg L^{-1} and the Fe^0 dosage of 5 g L^{-1} ; in Fig. 3C for Methyl Orange with the initial concentration of 50 mg L^{-1} and the Fe^0 dosage of 2 g L^{-1} . The degradation of Orange I and Orange II should be described as the first-order kinetic model, while the degradation of Methyl Orange should be described as the zeroth-order kinetic model. The first-order kinetic constants (k_1) for Orange I and Orange II and the zeroth-order kinetic constant (k_0) for Methyl Orange are listed in Table 1. The results showed that the k_1 or k_0 values all decreased with the increase in the initial pH value. Obviously, the lower pH was favorable for the reductive degradation of these azo dyes by Fe^0 . When the initial pH value decreased from 6.0 to 4.0, the k_1 values for Orange I and

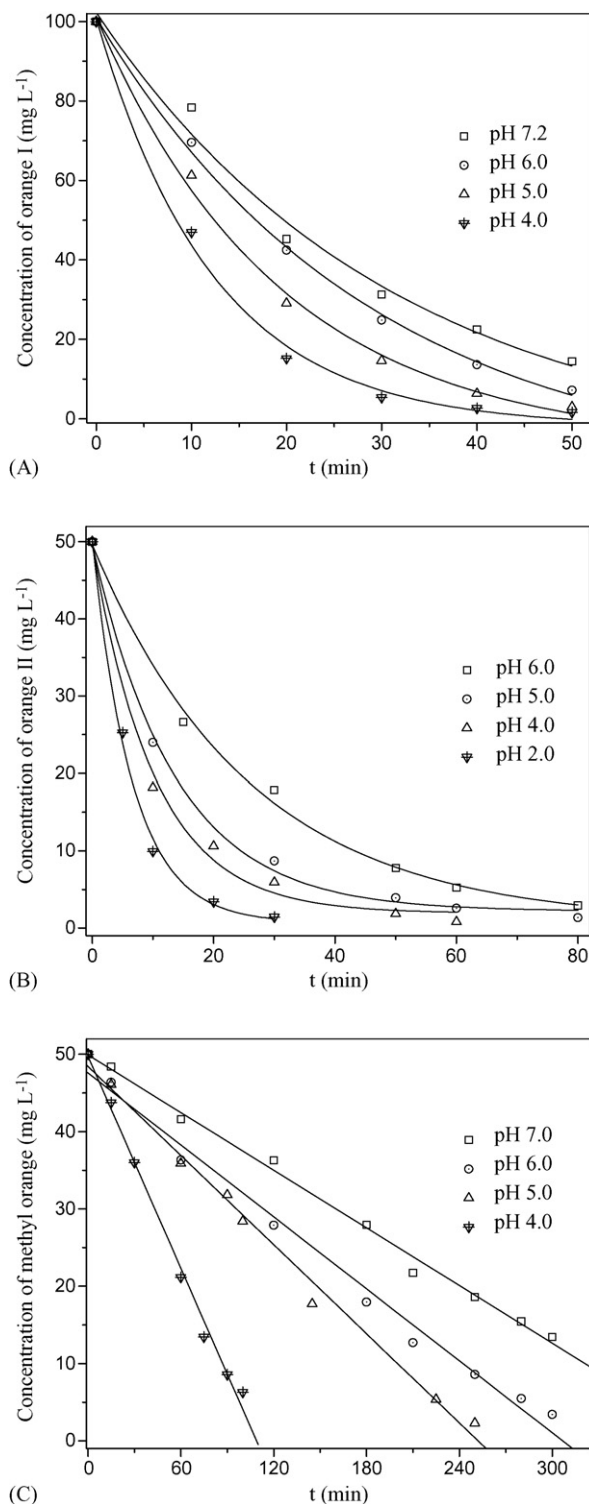


Fig. 3. The degradation of azo dyes under different initial pH value for Orange I (A): Fe⁰ dosage, 2 g L⁻¹; initial concentration, 100 mg L⁻¹; for Orange II (B): Fe⁰ dosage, 5 g L⁻¹; initial concentration, 50 mg L⁻¹; for Methyl Orange (C): Fe⁰ dosage, 2 g L⁻¹; initial concentration, 50 mg L⁻¹.

Orange II could enhance about 1.6 and 1.8 times, respectively. Because H⁺ should be involved in the reductive reaction by Fe⁰, the increase in the concentration of H⁺ would enhance obviously the reduction of azo dyes [3,6]. And the lower pH should

Table 1

The first-order kinetic constants (k_1) for Orange I and Orange II, and the zeroth-order kinetic constant (k_0) for Methyl Orange at different initial pH value

	pH 4.0	pH 5.0	pH 6.0	pH 7.2
Orange I				
k_1 ($\times 10^{-3}$ min ⁻¹)	86.4	71.4	53.1	39.4
R	0.993	0.998	0.996	0.996
	pH 2.0	pH 4.0	pH 5.0	pH 6.0
Orange II				
k_1 ($\times 10^{-3}$ min ⁻¹)	119.0	65.2	44.8	35.9
R	0.990	0.996	0.993	0.998
	pH 4.0	pH 5.0	pH 6.0	pH 7.0
Methyl Orange				
k_0 (mg L ⁻¹ min ⁻¹)	0.46	0.19	0.16	0.12
R	0.996	0.996	0.994	0.997

be helpful to remove the iron surface oxidation layer, and then enhance the reaction on the surface of iron powder.

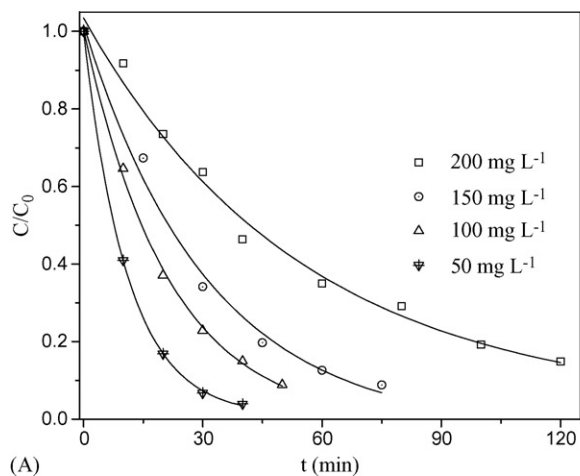
3.3. Effect of the initial concentrations

The effect of the initial concentration on the degradation kinetic constants is shown in Fig. 4A for Orange I with the Fe⁰ dosage of 2 g L⁻¹ at pH 7.0; in Fig. 4B for Orange II with the Fe⁰ dosage of 5 g L⁻¹ at pH 4.0; in Fig. 4C for Methyl Orange with the Fe⁰ dosage of 2 g L⁻¹ at pH 4.0. For Orange I, the initial concentrations of 50, 100, 150 and 200 mg L⁻¹ were selected; and for Orange II, the initial concentrations of 50, 100, 200 and 300 mg L⁻¹ were selected; while for Methyl Orange, initial concentrations of 20, 50, 150 and 200 mg L⁻¹ were used. The first-order kinetic constants (k_1) for Orange I and Orange II and the zeroth-order kinetic constant (k_0) for Methyl Orange are listed in Table 2. The experimental results showed that the degradation kinetic constants for Orange I and Orange II decreased with the increase in their initial concentration but the degradation kinetic constant for Methyl Orange obviously increased with the

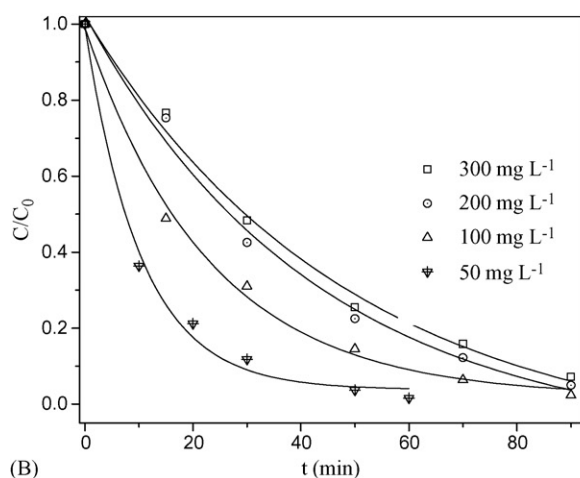
Table 2

The first-order kinetic constants (k_1) for Orange I and Orange II, and the zeroth-order kinetic constant (k_0) for Methyl Orange with different initial concentration of azo dyes

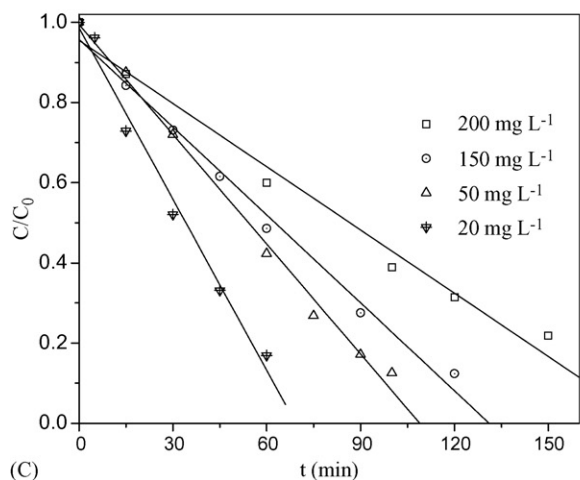
	50	100	150	200
Orange I (mg L ⁻¹)				
k_1 ($\times 10^{-3}$ min ⁻¹)	82.6	48.5	33.7	16.2
R	0.996	0.999	0.996	0.995
	50	100	200	300
Orange II (mg L ⁻¹)				
k_1 ($\times 10^{-3}$ min ⁻¹)	65.2	40.4	33.3	29.3
R	0.996	0.998	0.996	0.996
	20	50	150	200
Methyl Orange (mg L ⁻¹)				
k_0 (mg L ⁻¹ min ⁻¹)	0.28	0.46	1.1	1.1
R	0.994	0.996	0.995	0.992



(A)



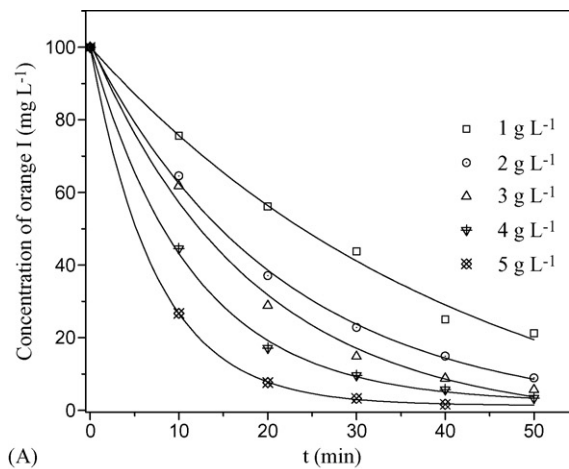
(B)



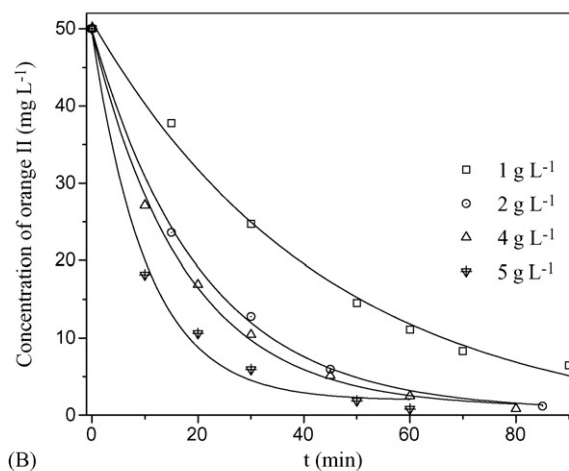
(C)

Fig. 4. The degradation of azo dyes with different initial concentration for Orange I (A): Fe^0 dosage, 2 g L^{-1} , pH 7.0; for Orange II (B): Fe^0 dosage, 5 g L^{-1} , pH 4.0; for Methyl Orange (C) Fe^0 dosage, 2 g L^{-1} , pH 4.0.

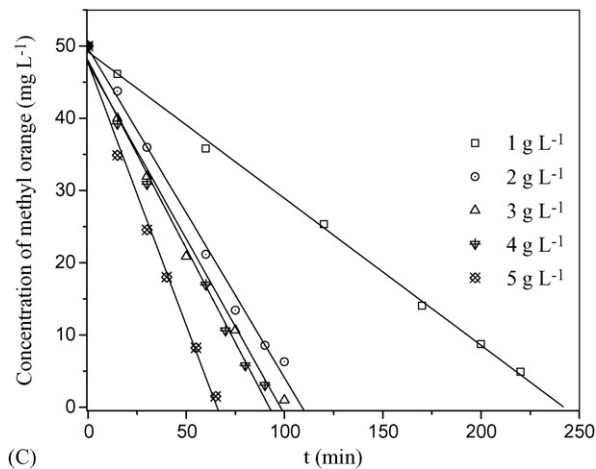
increase in its initial concentration. At pH 4.0, the kinetic constants of Orange II increased up to about two times when the initial concentration decreased from 200 to 50 mg L^{-1} . However, that of Orange I increased up to about five times when the initial concentration decreased from 200 to 50 mg L^{-1} .



(A)



(B)



(C)

Fig. 5. The degradation of azo dyes with different dosage of Fe^0 for Orange I (A): initial concentration, 100 mg L^{-1} , pH 7.0; for Orange II (B): initial concentration, 50 mg L^{-1} , pH 4.0; for Methyl Orange (C): initial concentration, 50 mg L^{-1} , pH 4.0.

3.4. Effect of Fe^0 dosage

The effect of the Fe^0 dosage on the reduction kinetic constants is shown in Fig. 5A for Orange I in the initial concentration of 100 mg L^{-1} at pH 7.0; in Fig. 5B for Orange II in the

Table 3

The first-order kinetic constants (k_1) for Orange I and Orange II, and the zeroth-order kinetic constant (k_0) for Methyl Orange with different Fe^0 dosage (g L^{-1})

	1	2	3	4	5
Fe ⁰ dosage (g L^{-1}) for Orange I					
k_1 ($\times 10^{-3} \text{ min}^{-1}$)	32.3	48.5	59.8	67.9	103
R	0.992	0.999	0.996	0.992	0.990
	1	2		4	5
Fe ⁰ dosage (g L^{-1}) for Orange II					
k_1 ($\times 10^{-3} \text{ min}^{-1}$)	24.3	44.1		50.2	65.2
R	0.994	0.999		0.999	0.996
	1	2	3	4	5
Fe ⁰ dosage (g L^{-1}) for Methyl Orange					
k_0 ($\text{mg L}^{-1} \text{ min}^{-1}$)	0.20	0.46	0.49	0.52	0.73
R	0.999	0.996	0.994	0.996	0.996

initial concentration of 50 mg L^{-1} at pH 4.0; in Fig. 5C for Methyl Orange I in the initial concentration of 50 mg L^{-1} at pH 4.0. The first-order kinetic constants (k_1) for Orange I and Orange II and the zeroth-order kinetic constant (k_0) for Methyl Orange with different Fe^0 dosage are listed in Table 3. The results showed the degradation kinetic constants for Orange I, Orange II and Methyl Orange obviously increased with the increase in the Fe^0 dosage. When the Fe^0 dosage increased from 1 to 5 g L^{-1} , the first-order kinetic constants of Orange I and Orange II increased about 3.2 and 2.6 times, respectively, while the zeroth-order kinetic constant of Methyl Orange increased about 3.6 times. The higher Fe^0 dosage should favor the degradation of Orange I, Orange II and Methyl Orange by Fe^0 .

3.5. Discussion on the effect of substituent groups

On the basis of the experimental results above, the degradation of azo dyes should strongly depend on the chemical structure and substituent groups. It is well known that amines ($-\text{NH}_2$, $-\text{NHR}$ and $-\text{NR}_2$) and hydroxyl group are very strongly active *ortho* and *para* directors with nonbonding electrons [13]. Generally, these electron-donating substituent groups inductively take electron density from the ring while giving electron density back by resonance, and they interact with the ring through their 2p orbital overlapping with the 2p orbital of a ring carbon [13]. Amines ($-\text{NH}_2$, $-\text{NHR}$ and $-\text{NR}_2$) and hydroxyl group in azo dye may result in different properties and degradation mechanisms when these groups are connected with phenol or naphthols. Thus, the effects of chemical structures and substituent groups on the degradation of azo dyes have attracted much attention in the field of photodegradation, chemical oxidation and anaerobic biodegradation process for the removal of azo dyes in recent years [8,10,14–16].

To disclose the effect of substituent groups, reductive mechanisms should be discussed. As shown in Fig. 1, Orange I

and Orange II contain a hydroxyl group conjugated with azo-linkage and usually exist an equilibrium mixture of two tautomeric forms (azo or hydrazone) in the aqueous solution [1,2]. It was reported that the hydrazone form should be favorable at equilibrium in aqueous medium when the hydroxyl group should be positioned in a naphthol *ortho* to the azo bond of azo dyes (such as, Orange I). Thus, for Orange II, the intramolecular hydrogen bonding could be formed in the solution [17–19]. Different from Orange I and Orange II, Methyl Orange is derived from the *p*-dimethylaminoaniline group linked with azo bond. Firstly, the larger conjugated π system of naphthalene ring (conjugated energy: 255 kJ mol^{-1}) is more favorable than the smaller conjugated π system of benzene ring (conjugated energy: 152 kJ mol^{-1}) through resonance for the delocalization of the nonbonding electron pairs of substituent groups and nitrogen in the azo bond. Secondly, the naphthol in the chemical structures of Orange I and Orange II may have a stronger influence on the azo bond than the *p*-dimethylaminoaniline group when the powerful electron withdrawing sulfonate group exists in the monoazo dyes. Consequently, the N–N cleavage of Orange I and Orange II may be comparatively easier than that of Methyl Orange. Based on the previous literatures [3–5,12,19,20], the suggested degradation pathways of Orange I, Orange II and Methyl Orange through the cleavage of the azo bond by the reductive processes are shown in Fig. 6. The HPLC–MS analyses of the main intermediates of azo dyes are shown in Fig. 7. The results in Fig. 7A shows that sulfanilic acid was the same intermediate derived from the reduction degradation of Orange I, Orange II and Methyl Orange because the same obvious negative peak with m/z ratio of 172 was detected, which is consistent with for sulfanilic acid $[\text{M}-\text{H}]^-$. The positive ion with m/z ratio of 157 in Fig. 7B was ascribed to aminonaphthoquinones [21], which might be in the equilibria state with amino-naphthols. Based on the chemical structure, the second intermediate was 1-amino-4-naphthol for Orange I, while that was 1-amino-2-naphthol for Orange II. The positive ion peak with m/z ratio of 137 for Methyl Orange in Fig. 7C was assigned to *p*-dimethylaminoanilinium, which might be due to the second intermediate (*p*-dimethylaminoaniline) for Methyl Orange.

Generally, the L–H model was usually used for describing the surface reaction and could be simplified into the first-order kinetic model when only a small number of reactive surface sites were occupied and the concentrations of the reactants were low. When the reactive surface sites were saturated or played the minor role in the reaction, the reaction might follow the zeroth-order kinetic model [20]. As shown in Fig. 1, the pK_a value of Methyl Orange ($\text{pK}_a = 3.7$) is much lower than those of Orange I ($\text{pK}_a = 8.2$) and Orange II ($\text{pK}_a = 11.4$). In the experiments, especially in the pH beyond 4.0, the sulfonate group of Methyl Orange might exist mainly with the anionic form, while the sulfonate groups of Orange I and Orange II might exist mainly with the sulfonic acid form which might be favorable for the adsorption onto the surface hydroxyls of iron-oxides or hydroxides of the Fe^0 powder. There were several reports about the adsorption of azo dyes onto the surface hydroxyls of metal-oxides or hydroxides, and it was suggested that the adsorption

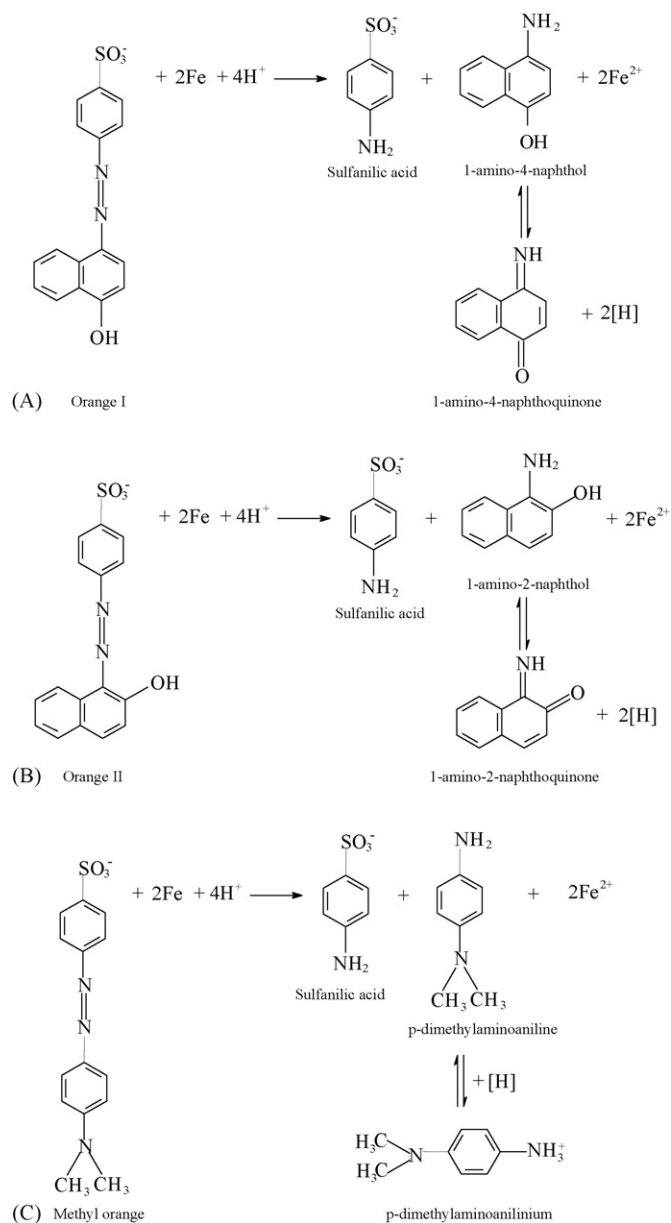


Fig. 6. The suggested degradation pathway of Orange I (A), Orange II (B) and Methyl Orange (C) by Fe^0 .

might have some influences on the degradation of azo dyes by catalytic oxidation or reduction, leading to the first-order kinetic behavior of the degradation of azo dyes and higher degradation rates, which was coincidence with the experimental results. As for Methyl Orange, its adsorption might play minor role in the reductive process, then resulting in the zeroth-order kinetic behavior.

The UV–vis absorption spectra of the diluted reaction solutions of Orange I, Orange II and Methyl Orange by Fe^0 were recorded, as shown in Fig. 8. For Orange I, the strong absorbance band at 477 nm was ascribed to the $n-\pi^*$ transition of the azo bond, and other bands at 238, 266 and 289 nm and the shoulder at 331 nm were attributable to the $\pi-\pi^*$ transition related to aromatic rings [2,20]. After 10 min treatment by Fe^0 , the UV–vis

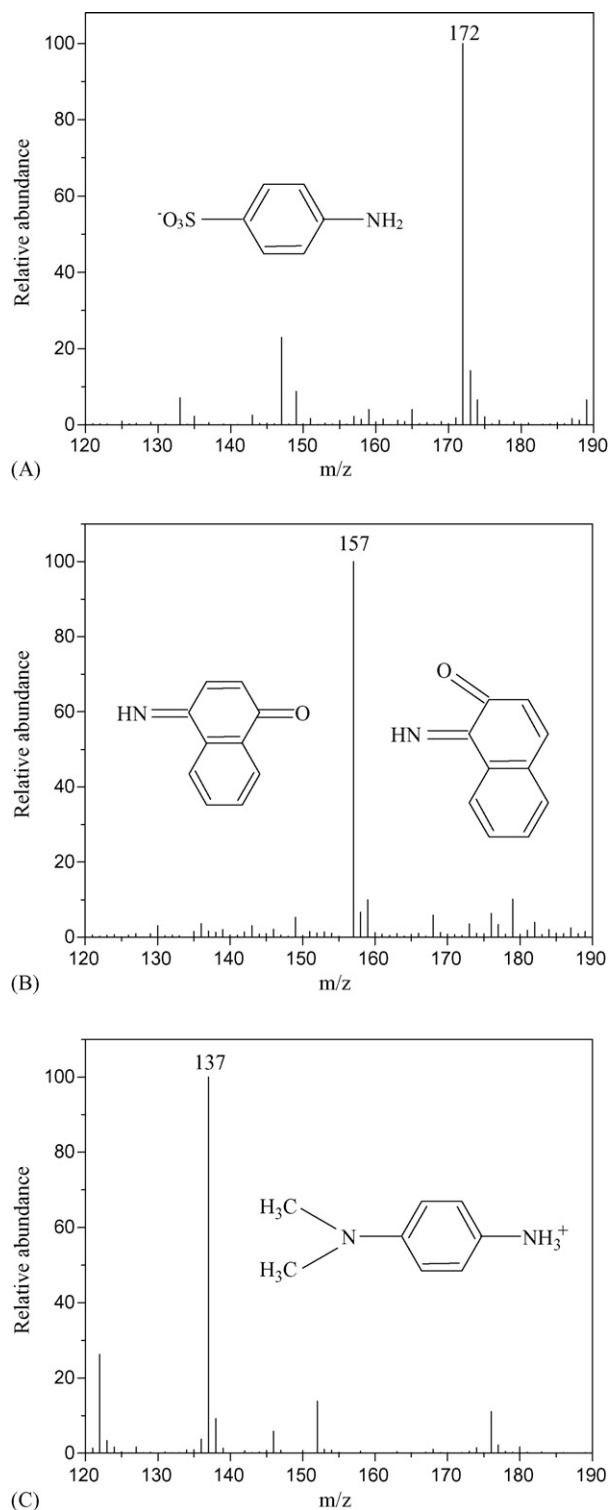


Fig. 7. The mass spectra for the intermediates including sulfanilic acid for three kinds of dyes (A), amino quinones for Orange I and Orange II (B) and *p*-dimethylaminoanilinium (C) for Methyl Orange (initial concentration of dyes, 50 mg L^{-1} ; Fe^0 dosage, 2 g L^{-1} , pH 4.0).

absorption spectra of reaction solutions showed the decrease of the bands at 477 and 289 nm and the disappearance of the band at 266 nm, which suggested the degradation of Orange I and the formation of very unstable intermediates. With the ongoing of

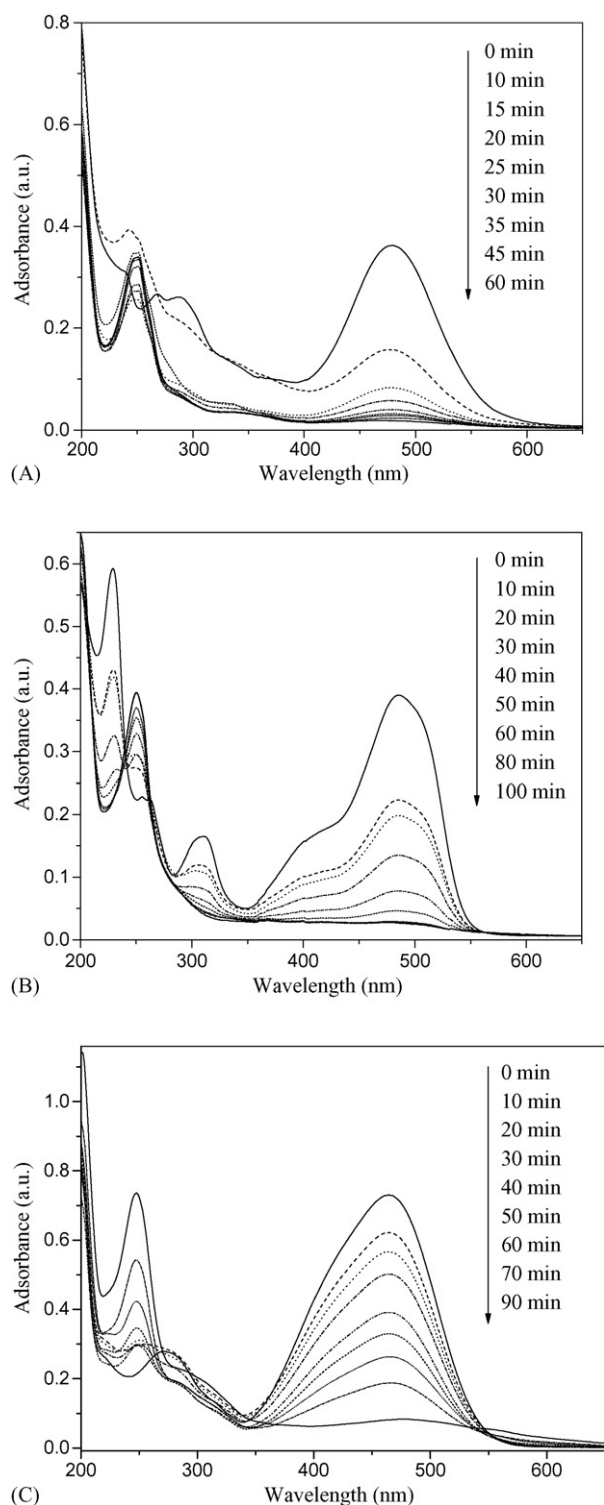


Fig. 8. The UV-vis absorption spectra for Orange I (A), Orange II (B) and Methyl Orange (C) (initial concentration of azo dyes, 50 mg L^{-1} , pH 4.0; Fe^0 dosage, 5 g L^{-1}).

the experiment, the UV-vis absorption spectra showed the gradual disappearance of the band at 477 nm and the appearance of bands at 246 , 251 and 340 nm , which indicated the produce of 1-amino-4-naphthol as the major intermediate of the degradation of Orange I [20].

As shown in Fig. 8B, there was a strong absorbance band at 483 nm due to the $n-\pi^*$ transition of the azo bond of Orange II, and other bands at 308 and 228 nm , and a doublet at 261 and 254 nm were attributed to the $\pi-\pi^*$ transition related to aromatic rings of Orange II [1,3,22]. After 10 min reaction, the bands at 483 , 308 and 228 nm decreased, and the doublet at 261 and 254 nm disappeared, but the band at 250 nm appeared, which also suggested the degradation of Orange II and the formation of very unstable intermediates. Obviously, the band at 250 nm increased gradually from 10 to 80 min , and then decreased beyond 80 min , which indicated the formation and degradation of 1-amino-2-naphthol as the major intermediate during the degradation of Orange II [3].

As shown in Fig. 8C, for Methyl Orange, the strong absorbance band at 464 nm is assigned to the azo band under the strong influence of the electron-donating dimethylamino group, and the band at 270 nm is ascribed to the $\pi-\pi^*$ transition related to aromatic rings [23]. After 10 min reaction, the band at 464 nm decreased, and the band at 270 nm disappeared, but the band at 247 nm appeared. Comparison with the band at 280 nm for aniline, the electron-donating dimethylamino group at the *para* position of aniline might lead to the blue shift and then the band attributed to *p*-dimethylaminoaniline might be below 280 nm . Thus, the band at 247 nm of the reaction solution increased gradually, which might be attributable to *p*-dimethylaminoaniline.

The FTIR results are shown in Fig. 9 for the original Fe^0 powder, the Fe^0 powder after 2 h reaction of Orange I, Orange II and Methyl Orange. The band at 1641 cm^{-1} was attributable to the adsorbed water, the weak broad band at 910 cm^{-1} was ascribed to polymeric $\text{Fe}(\text{OH})_2$ and the weak bands at 1034 and 751 cm^{-1} was attributable to the $\delta\text{-OH}$ and $\gamma\text{-OH}$ bending vibrations of a small amount of lepidocrocite ($\gamma\text{-FeOOH}$) on the surface of the original Fe^0 powder [24]. After 2 h reaction with azo dyes, the band at 1023 cm^{-1} attributed to lepidocrocite increased obviously. The board band at 898 cm^{-1} might be ascribed to akaganeite ($\beta\text{-FeOOH}$) and polymeric $\text{Fe}(\text{OH})_2$ [24]. It is suggested that the coating of iron oxides or hydroxides might

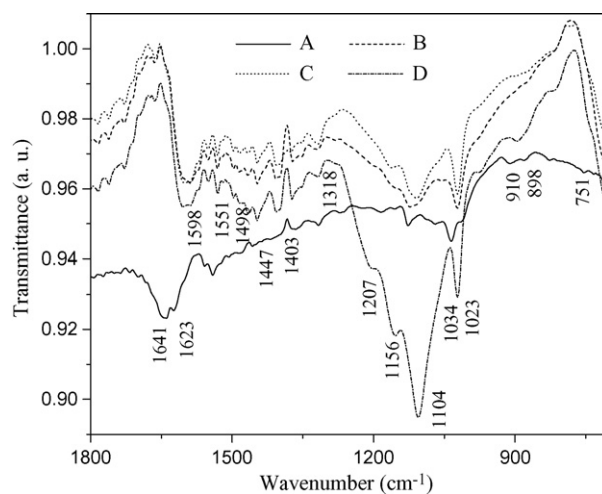


Fig. 9. FTIR of the original Fe^0 powder (A) and the Fe^0 powder after 2 h reaction for Orange I (B), Orange II (C) and Methyl Orange (D) (initial concentration of azo dyes, 50 mg L^{-1} , pH 4.0; Fe^0 dosage, 5 g L^{-1}).

be formed on the surface of iron powder during the degradation of azo dyes by Fe^0 .

The bands of 1447, 1498, 1551, 1598 and 1623 cm^{-1} were assigned to C=C aromatic skeleton vibrations, while the bands at 1403 and 1318 cm^{-1} were ascribed to the O=H bending vibrations and deformation [7,9,25]. After 2 h reaction, there was not the intense band at 1514 cm^{-1} attributed to the —N=N— bond vibrations or to aromatic ring vibrations, or to the bending vibration mode $\delta(\text{N—H})$ of the hydrazone form, which suggested that the azo bonds of Orange I, Orange II and Methyl Orange were completely degraded by Fe^0 in the experiments. The strong bands at 1104, 1156 and 1207 cm^{-1} were assigned to the symmetric and asymmetric stretching of sulfonate anions (—SO_3^-) of benzene ring [26–28], which might be ascribed to sulfanilic acid, indicating that the strong adsorption of sulfanilic acid was formed on the colloid coating of iron-oxides or hydroxides on the surface of Fe^0 .

4. Conclusion

Orange I, Orange II and Methyl Orange could be effectively reduced by Fe^0 , and the initial degradation rate followed the order as Orange I > Orange II > Methyl Orange under the same experimental conditions. The degradation of Orange I and Orange II could be described by the first-order kinetic model, while the degradation of Methyl Orange could be described by the zeroth-order kinetic model. The degradation kinetic constants of Orange I, Orange II and Methyl Orange increased with the increase in the Fe^0 dosage and with the decrease in the pH value. Sulfanilic acid was the same intermediate, while the second intermediate was 1-amino-4-naphthol for Orange I, 1-amino-2-naphthol for Orange II and *p*-dimethylaminoaniline for Methyl Orange. It should be concluded that the reductive degradation by zerovalent iron strongly depends on the effect of substituent groups.

Acknowledgements

The authors would like to thank the National Natural Science Foundation of China (No. 20577007), Foundation of Natural Science of Guangdong Province (No. 04002223) and Guangdong Technological Foundation (No. 2004B33301014) for financial supports to this work.

References

- [1] L.C. Abbott, S.N. Batchelor, J. Oakes, B.C. Gilbert, A.C. Whitwood, J.R.L. Smith, J.N. Moore, Experimental and computational studies of structure and bonding in parent and reduced forms of the azo dye Orange II, *J. Phys. Chem. A* 109 (2005) 2894–2905.
- [2] K.K. Sharma, P. O'Neill, J. Oakes, S.N. Batchelor, B.S. Madhava Rao, One-electron oxidation and reduction of different tautomeric forms of azo dyes: a pulse radiolysis study, *J. Phys. Chem. A* 107 (2003) 7619–7628.
- [3] J.A. Mielczarski, G.M. Atenas, E. Mielczaeski, Role of iron surface oxidation layers in degradation of azo-dye water pollutants in weak acidic solutions, *Appl. Catal. B: Env.* 56 (2005) 289–303.
- [4] S. Nam, P.G. Tratnyek, Reduction of azo dyes with zero-valent iron, *Wat. Res.* 34 (2000) 1837–1845.
- [5] H. Zhang, L.J. Duan, Y. Zhang, F. Wu, The use of ultrasound to enhance the decolorization of the C. I. Acid Orange 7 by zero-valent iron, *Dyes Pigments* 65 (2005) 39–43.
- [6] T. Suzuki, S. Timofei, L. Kurunczi, U. Dietze, G. Schüümann, Correlation of aerobic biodegradability of sulfonated azo dyes with the chemical structure, *Chemosphere* 45 (2001) 1–9.
- [7] L. Lucarelli, V. Nadochenko, J. Kiwi, Environmental photochemistry: quantitative adsorption and FTIR studies during the TiO_2 -photocatalyzed degradation of Orange II, *Langmuir* 16 (2000) 1102–1108.
- [8] V. Augugliari, C. Baiocchi, A.B. Prevot, E. García-López, V. Loddo, S. Malato, G. Marci, L. Palmisano, M. Pazzi, E. Pramauro, Azo-dyes photocatalytic degradation in aqueous suspension of TiO_2 under solar irradiation, *Chemosphere* 49 (2002) 1223–1230.
- [9] K. Bourikas, M. Styliidi, D.I. Kondarides, X.E. Verykios, Adsorption of Acid Orange 7 on the surface of titanium dioxide, *Langmuir* 21 (2005) 9222–9230.
- [10] Y. Yang, Q.Y. Wu, Y.H. Guo, C.W. Hu, E.B. Wang, Efficient degradation of dye pollutants on nanoporous polyoxotungstate-anatase composite under visible-light irradiation, *J. Mol. Catal. A: Chem.* 225 (2005) 203–212.
- [11] J. Oakes, P. Gratton, Kinetic investigations of azo dye oxidation in aqueous media, *J. Chem. Soc., Perkin Trans. 2* (1998) 1857–1864.
- [12] A.S. Özen, V. Aviyente, F. De Proft, P. Geerlings, Modeling the substituents effect on the oxidative degradation of azo dyes, *J. Phys. Chem. A* 108 (2004) 5990–6000.
- [13] R.J. Ouellette, *Organic Chemistry, A Brief Introduction*, Macmillan Publishing Company, New York, 1994.
- [14] A. Zille, P. Ramalho, T. Tzanov, R. Millward, V. Aires, M.H. Cardoso, M.T. Ramalho, G.M. Gübitz, A. Cavaco-Paulo, Predicting dye biodegradation from redox potentials, *Biotechnol. Prog.* 20 (2004) 1588–1592.
- [15] P.A. Ramalho, M.H. Cardoso, A. Cavaco-Paulo, M.T. Ramalho, Characterization of azo reduction activity in a novel ascomycete yeast strain, *Appl. Env. Microbiol.* 70 (2004) 2279–2288.
- [16] C. Guillard, H. Lachheb, A. Houas, M. Ksibi, E. Elaloui, J.-M. Hermann, Influence of chemical structure of dyes, of pH and of inorganic salts on their photocatalytic degradation by TiO_2 comparison of the efficiency of powder and supported TiO_2 , *J. Photochem. Photobiol. A: Chem.* 158 (2003) 27–36.
- [17] A.C. Olivieri, R.B. Wilson, I.C. Paul, D.Y. Curtin, ^{13}C NMR and X-ray structure determination of 1-(aryloxy)-2-naphthols. Intramolecular proton transfer between nitrogen and oxygen atoms in solid state, *J. Am. Chem. Soc.* 111 (1989) 5525–5532.
- [18] J.O. Morley, O.J. Guy, M.H. Charlton, Molecular modeling studies on the photochemical stability of azo dyes, *J. Phys. Chem. A* 108 (2004) 10542–10550.
- [19] T. Stanoeva, D. Neshechadin, G. Gescheidt, J. Ludvik, B. Lajoie, S.N. Batchelor, An investigation into the initial degradation steps of four major dye chromophores: study of their one-electron oxidation and degradation by EPR, ENDOR, cyclic voltammetry, and theoretical calculations, *J. Phys. Chem. A* 109 (2005) 11103–11109.
- [20] G.M. Atenas, E. Mielczaeski, J.A. Mielczarski, Remarkable influence of surface composition and structure of oxidized iron layer on Orange I degradation mechanisms, *J. Colloid Interface Sci.* 289 (2005) 171–183.
- [21] F.P. van der Zee, I.A.E. Bisschops, V.G. Blanchard, R.H.M. Bouwman, G. Lettinga, J.A. Field, The contribution of biotic and abiotic processes during azo dye reduction in anaerobic sludge, *Wat. Res.* 37 (2003) 3098–3109.
- [22] R.L. Reeves, M.S. Magglo, S.A. Harkaway, A critical spectrophotometric analysis of the dimerization of some ionic azo dyes in aqueous solution, *J. Phys. Chem.* 83 (1979) 2359–2368.
- [23] C. Galindo, P. Jacques, A. Kalt, Photodegradation of the aminoazobenzene Acid Orange 52 by three advanced oxidation processes: UV/ H_2O_2 , UV/ TiO_2 and vis/ TiO_2 , comparative mechanistic and kinetic investigations, *J. Photochem. Photobiol. A: Chem.* 130 (2000) 35–47.
- [24] R.M. Cornell, U. Schwertmann, *The Iron Oxides Structure, Properties, Reactions, Occurrences and Uses*, Wiley-VCH Verlag GmbH & Co. KGaA, Weinheim, 2003.
- [25] J. Bandara, J.A. Mielczarski, J. Kiwi, 2. Photosensitized degradation of azo dyes on Fe, Ti, and Al oxides. Mechanism of charge transfer during the degradation, *Langmuir* 15 (1999) 7680–7687.

- [26] G. Zundel, Hydration and Intermolecular Interaction, Academic Press, New York, 1969.
- [27] N.B. Colthup, L.H. Daly, S.E. Wiberley, Introduction to Infrared and Raman Spectroscopy, second ed., Academic Press, New York, 1975.
- [28] W.J. Chen, J.A. Sauer, M. Hara, The effect of ion cross-links on the deformation behavior of homoblends made of poly(styrene-*co*-styrenesulfonic acid) and poly(styrene-*co*-4-vinylpyridine), *Polymer* 44 (2003) 7729–7738.